

Constraints on Dark Matter Models from Supermassive Black Hole Evolution

John Ellis,^{1,2,*} Malcolm Fairbairn,^{1,†} Juan Urrutia,^{3,4,‡} and Ville Vaskonen^{3,5,6,§}

¹*King's College London, Strand, London, WC2R 2LS, United Kingdom*

²*Theoretical Physics Department, CERN, Geneva, Switzerland*

³*Keemilise ja Bioloogilise Füüsika Instituut, Rävala pst. 10, 10143 Tallinn, Estonia*

⁴*Department of Cybernetics, Tallinn University of Technology, Akadeemia tee 21, 12618 Tallinn, Estonia*

⁵*Dipartimento di Fisica e Astronomia, Università degli Studi di Padova, Via Marzolo 8, 35131 Padova, Italy*

⁶*Istituto Nazionale di Fisica Nucleare, Sezione di Padova, Via Marzolo 8, 35131 Padova, Italy*

A semi-analytical model for the evolution of galaxies and supermassive black holes (SMBHs) within the Λ CDM paradigm has been shown to yield stellar mass-BH mass relations that reproduce both the JWST and pre-JWST observations. Either fuzzy or warm dark matter (FDM or WDM) would suppress the formation of the smaller galactic halos that play important roles in the CDM fit to the high-redshift SMBH data. Our analysis of the stellar mass-BH mass relation disfavors FDM fields with masses $< 2.0 \times 10^{-20}$ eV and WDM particles with masses < 7.2 keV, both at the 95% confidence level.

KCL-PH-TH/2025-37, CERN-TH-2025-186, AION-REPORT/2025-07

Introduction – The advent of the James Webb Space Telescope (JWST) has enabled surveys to probe the infrared universe with unprecedented accuracy [1–8], facilitating exploration of the reionization era and before (see [9] for a review). One of the most interesting developments has been new insight into proposed mechanisms for the formation of supermassive black holes (SMBHs) [10]. It had been suggested that they could have been seeded by black holes (BHs) with masses $\mathcal{O}(10^2 - 10^3)M_\odot$ that could be the remnants of population III (Pop-III) [11] stars that collapsed at redshifts $z \gtrsim 10$ (light-seed scenario), or by heavier BHs with masses $\mathcal{O}(10^5)M_\odot$ in the cores of protogalaxies that subsequently merged to form the larger galaxies seen at lower redshifts (heavy-seed scenario).

Using JWST, a new population of high- z BHs has been discovered [12–20] that represent a challenge for the conventional picture of SMBH formation [21–24]. The high- z SMBHs seem to require either a heavy-seed scenario [25–27] or a very high efficiency for mergers of light seeds [28, 29] in order for them to be a viable option. The possibility of growth through mergers inside nuclear clusters has also been tested against the JWST results [30]. An active topic of debate has been whether these SMBHs are accreting at super-Eddington rates, in which case their masses may have been overestimated [31–35]. In parallel, the discovery of ‘little red dots’ [36–39] has defied many astrophysical assumptions about galaxies at high z [40–42]. There is an active debate centered around the nature of these objects and the role that SMBHs play in them [43–47].

This work explores the evolution of SMBH seeds in CDM, FDM, and WDM universes, building on our ear-

lier results for the star formation rate [48] and our semianalytical model for the coevolution of galaxies and SMBHs [28]. We compare model predictions to the stellar mass-BH mass observations across a broad redshift range and conclude that, despite its uncertainties, SMBH evolution is a sensitive probe of DM properties, indeed more powerful than the stellar UV luminosity functions that we studied previously [48]. The reason is that the bright stars that dominate the UV emission are short-lived, so the UV luminosity function serves as a cosmic “snapshot” in which the lightest halos are too dim to be probed. In contrast, SMBHs are long-lived, carrying information from as early as $z \sim 20$ when they were first formed in light halos, which are very sensitive to the nature of DM.

We show here that the best-fit parameters for the evolution of the SMBH population in the CDM model are well within the ranges expected from simulations and physical arguments, making the observed SMBH population less surprising than previously thought. We further conclude that the current population of SMBHs disfavors FDM fields with masses $< 2.0 \times 10^{-20}$ eV and WDM particles with masses < 7.2 keV, both at the 95% confidence level. Finally, for the light-seed scenario to be viable, it requires the buildup of light halos, making the light-seed case more sensitive to the nature of DM. This correlation between the nature of DM and the origin of SMBHs, will provide an interesting phenomenology for future gravitational wave detectors like LISA [49] or AION [50], which we plan to explore in future work.

SMBH evolution and galactic feedback – To evolve the DM structures, galaxies and SMBHs, we follow the approach derived in [28], which is based on an empirical estimate of the star formation rate, a parametrization of the SMBH accretion rate that accounts for feedback effects, and the growth rate of galaxies and SMBHs estimated from the Extended Press-Schechter (EPS) formalism for an elliptical collapse barrier. The average stellar

* john.ellis@cern.ch

† malcolm.fairbairn@kcl.ac.uk

‡ juan.urrutia@kbfi.ee

§ ville.vaskonen@pd.infn.it

masses and SMBH masses M_J ($J = *, \text{BH}$) in DM halos of mass M evolve by mergers from redshift $z' > z$ to z as

$$\Delta M_J^{\text{merg}}(M, z, z') = \int_0^M dM' M_J(M', z') \frac{dN(M, z, z')}{dM'} - M_J(M, z'), \quad (1)$$

where

$$\frac{dN(M, z, z')}{dM'} = \frac{M}{M'} \frac{dS}{dM'} p_{\text{FC}}(M', z'|M, z) \quad (2)$$

gives the number of progenitors of the halo of mass M in the mass range $(M', M' + dM')$. The function $S(M)$ is the variance of the matter fluctuations that depends on the DM model, and $p_{\text{FC}}(M', z'|M, z)$ is the first-crossing probability distribution with $M > M'$ and $z' > z$ that we evaluate using the fit that we derived in [48], which considers elliptical collapse and the DM dependence in the variance of matter perturbations. The growth rate through mergers, \dot{M}_J^{merg} , is obtained from the limit $z' \rightarrow z$. For the growth of the SMBHs via mergers, we consider

$$\dot{M}_{\text{BH}}^{\text{merg}}(M, p_{\text{BH}}) = \begin{cases} \dot{M}_{\text{BH}}^{\text{merg}}(M), & \dot{M}_{\text{BH}}^{\text{merg}}(M) < 0 \\ p_{\text{BH}} \dot{M}_{\text{BH}}^{\text{merg}}(M), & \dot{M}_{\text{BH}}^{\text{merg}}(M) \geq 0 \end{cases}, \quad (3)$$

where p_{BH} is a parameter characterising the probability that the BHs inside merging halos will themselves merge. Although considering a constant p_{BH} might be simplistic, it can be used to approximate different merging mechanisms. For example, nuclear star clusters would lead to $p_{\text{BH}} \simeq 1$ [51].

For the star formation rate (SFR), we adopt the best fit that we found in [48], derived from the HST and JWST UV luminosity function data. This fit is based on a parametrisation where the galaxy stellar mass grows proportional to the DM halo mass, $\dot{M}_* \propto \dot{M}$, with a proportionality factor that is a broken power-law as a function of the halo mass. The DM model dependence enters through the halo growth rate \dot{M} that we evaluate using the expression that we derived in [48].

In order to estimate the SMBH accretion, it is essential to understand the feedback mechanisms within a galaxy. We infer these from the effective SFR by expressing it as $\dot{M}_* = f_*(M) f_{\text{cold}}(M) f_B \dot{M}$ where $f_B = \Omega_B/\Omega_M \approx 0.16$ denotes the baryon fraction and $f_*(M) f_{\text{cold}}(M)$ is a broken power-law that peaks at $M = M_c$, given by

$$f_* f_{\text{cold}} = \epsilon \frac{\alpha + \beta}{\beta(M/M_c)^{-\alpha} + \alpha(M/M_c)^\beta} e^{-M_t/M}. \quad (4)$$

We found in [48] that the best-fit values for these parameters do not depend significantly on the DM model, and here we use the best-fit values found in the CDM model. We divide the broken power-law into the fraction of cold gas

$$f_{\text{cold}} \equiv \begin{cases} 1, & M < M_c \\ \dot{M}_*/(\epsilon f_B \dot{M}), & M \geq M_c \end{cases}, \quad (5)$$

and the SFR efficiency

$$f_* \equiv \epsilon \begin{cases} \dot{M}_*/(\epsilon f_B \dot{M}), & M < M_c \\ 1, & M \geq M_c \end{cases}. \quad (6)$$

The suppression of f_* at $M < M_c$ arises because supernova (SN) feedback depletes the cold gas, halting further star formation, while the suppression of f_{cold} at $M > M_c$ is caused by AGN feedback, which heats the gas in the galaxy. According to this interpretation, the remaining gas that can be accreted by the SMBH is

$$f_{\text{rem}} = 1 - (f_{\text{ej}} + f_*) f_{\text{cold}}, \quad (7)$$

where

$$f_{\text{ej}} \equiv (1 - f_*)(1 - f_{\text{SN}}) \begin{cases} 1, & M < M_c \\ f_{\text{cold}}^2, & M \geq M_c \end{cases}. \quad (8)$$

The quantity f_{SN} is the fraction of the gas left after star formation that is not expelled by the SN feedback. The motivation for introducing this parameter is to allow for some accretion on the SMBH at $M < M_c$, the halo mass which marks the transition from SN- to AGN-dominated feedback, and thus accommodate the low-mass AGNs seen by JWST. The solid curves in Fig. 1 show the gas fraction available for SMBH accretion at different redshifts. Below M_c , SMBHs can only accrete the fraction of gas not expelled by SN feedback, which in the case shown in Fig. 1 is $f_{\text{SN}} = 10^{-3}$. Following [52], we consider the accretion rate

$$\dot{M}_{\text{BH}}^{\text{acc}}(M_{\text{BH}}, M) = \min \left[f_{\text{Edd}} \dot{M}_{\text{Edd}}(M_{\text{BH}}), f_{\text{rem}} f_B (f_1^{\text{acc}} \dot{M} + f_2^{\text{acc}} M) \right], \quad (9)$$

where f_1^{acc} is a dimensionless parameter that describes the fraction of baryons accreted by the halo that, after star formation and internal feedback, are ultimately accreted onto the SMBH. In contrast, f_2^{acc} has units of inverse time and determines the rate at which the surrounding gas can be accreted. Finally, f_{Edd} is a dimensionless parameter that limits the total accretion rate as a fraction of the Eddington rate $\dot{M}_{\text{Edd}}(M_{\text{BH}})$.

The parameters of our model are summarized in Table 1. For each DM model, we begin by embedding a seed of mass m_{seed} at some redshift z_{seed} in every halo that is heavier than some minimal mass M_{seed} , and evolve the BH masses and stellar masses. In the above formalism we evolve only the expected BH mass, $M_{\text{BH}} = \int dP(m_{\text{BH}}) m_{\text{BH}}$. We assume that the occupation number is one as long as $M_{\text{BH}} > m_{\text{seed}}$ and in halos with $M_{\text{BH}} < m_{\text{seed}}$ the occupation number is less than one and the SMBH mass equals the seed mass. The occupation fraction can be expressed as

$$\frac{dP(m_{\text{BH}}|M_*, z)}{dm_{\text{BH}}} = \frac{M_{\text{BH}}(M_*, z)}{m_{\text{BH}}} \delta[m_{\text{BH}} - m_{\text{BH}}(M_*, z)]. \quad (10)$$

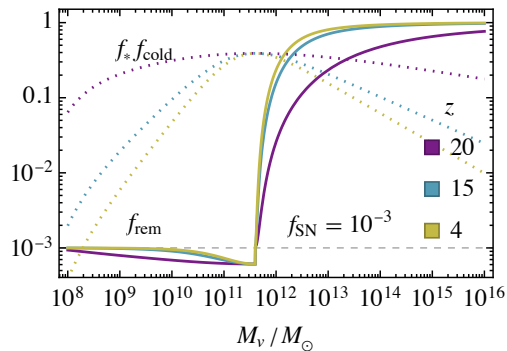


FIG. 1. The dotted curves in three colours corresponding to different redshifts show the SFR fitted to the UV luminosity function data, and the solid curves show the remaining gas fraction available for SMBH accretion at different redshifts.

Parameter	Interpretation
m_{seed}	Mass of the SMBH seed.
M_{seed}	Lowest halo mass that is planted with seeds.
p_{BH}	The probability that a halo merger ends in the merger of the central SMBHs.
f_{SN}	The fraction of gas that is not expelled after SN feedback.
f_{Edd}	The maximal allowed accretion as a fraction of the Eddington limit.
f_1^{acc}	The fraction of incoming baryons accreted onto the SMBH.
f_2^{acc}	The rate of accretion of baryons in the halo.
$m_{\text{FDM}}/\text{WDM}$	DM mass, if not CDM.

TABLE I. List of the parameters in our model and their interpretations.

We evolve numerically the galaxy stellar masses and the masses of their central SMBHs, resolving halos in the range $M_v = 10^2 - 10^{16} M_\odot$ and planting the seeds at $z = 20$. We have checked that our results are insensitive to this choice, and that the redshift steps and halo mass bins are small enough that the solutions are not affected.¹

In Fig. 2 we show the resulting stellar mass-BH mass relation at different redshifts for a benchmark case with $\log_{10}(m_{\text{seed}}/M_\odot) = 5$, $\log_{10}(M_{\text{seed}}/M_\odot) = 7.0$, $\log_{10} f_{\text{SN}} = -3.0$, $\log_{10} f_1^{\text{acc}} = -19.5$, $\log_{10}(f_2^{\text{acc}} \text{ Myr}) = -3.0$, $\log_{10} f_{\text{Edd}} = 0.5$ and $\log_{10} p_{\text{BH}} = -1$. We display results for two different cosmologies, CDM and FDM, with $m_{\text{FDM}} = 10^{-21} \text{ eV}$. We see in the lower panel that both DM models can approximately reproduce the observations at $z = 0$, but at high z , shown in the upper panel, the prediction is very sensitive to the DM model. There are two reasons for this. First, the abundance of low-mass halos is suppressed at the time of seeding for the non-CDM models and, secondly, at these masses, the

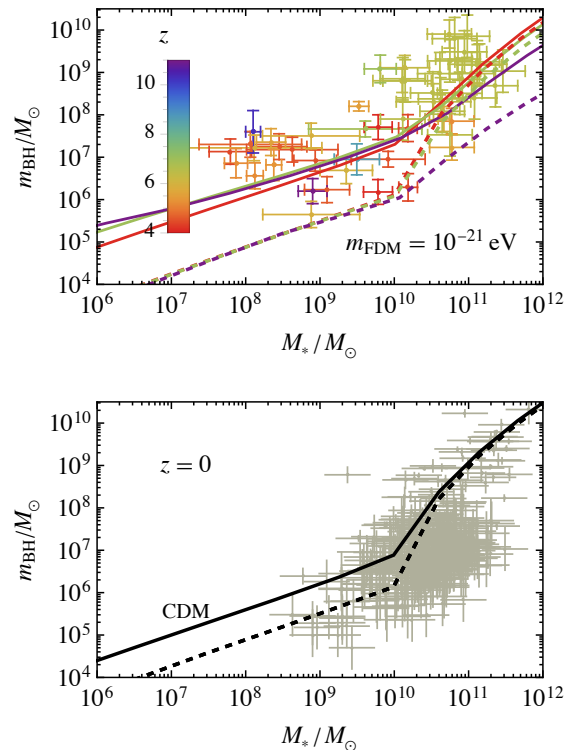


FIG. 2. Assuming a heavy-seed scenario, we show the different effects of FDM and CDM models on the growth of the seeds, and compare them with the observations of SMBHs and the stellar masses of the galaxies that host them. CDM calculations are shown as full lines and those in the FDM with mass $m_{\text{FDM}} = 10^{-21} \text{ eV}$ as dashed lines. The different colours in the top panel represent the different redshifts, while the lower panel represents the local universe, the SMBH mass-stellar mass measurements comes from [12–20, 54, 55].

SN feedback during reionisation makes accretion inefficient, so mergers at very high redshift can be the main channel for the growth of these SMBHs [53], which is further suppressed. The effect of WDM (not shown) is qualitatively similar to that of FDM. This example serves as an illustration of the suppression of the abundance of structures at small scales on the evolution of SMBHs.

In Fig. 3 we show the average evolution of an SMBH in a DM halo whose mass today is $M_v = 10^{13} M_\odot$. The blue curves show a heavy seed case, with the same values as for Fig. 2, and the orange curves are for a light seed case where we have taken $\log_{10}(m_{\text{seed}}/M_\odot) = 2.5$, $\log_{10}(M_{\text{seed}}/M_\odot) = 4.5$ and $p_{\text{BH}} = 1$. The solid, dashed and dotted curves correspond, respectively, to CDM, FDM with $m_{\text{FDM}} = 10^{-19} \text{ eV}$ and FDM with $m_{\text{FDM}} = 10^{-21} \text{ eV}$. We see that the growth curves are similar at low redshifts and that the heavy seed case grows steadily from $z = 12$, whereas in the CDM model, the light seed case shows more rapid growth at the beginning. The reason is that a large number of light halos are simultaneously trapped in a collapsing overdensity that becomes

¹ The complete evolution takes a few seconds in Mathematica on a M2 MacBook Air.

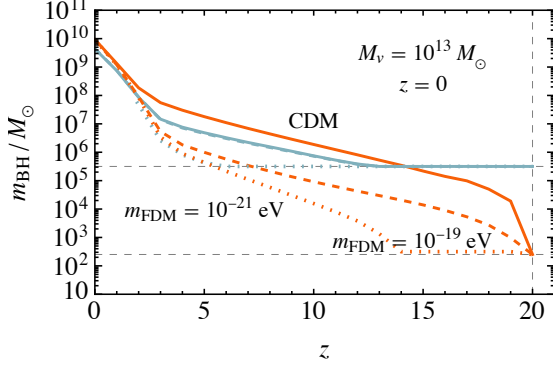


FIG. 3. Growth of individual SMBHs in both the light and heavy seed scenarios (blue and orange lines, respectively). CDM calculations are shown with solid curves and FDM with dashed ($m_{\text{FDM}} = 10^{-19}$ eV) and dotted ($m_{\text{FDM}} = 10^{-21}$ eV) curves. The host DM halo mass at $z = 0$ is fixed to $M_v = 10^{13} M_\odot$.

a heavy halo.² When looking at the dashed and dotted curves, we see that the FDM model leads to a slower SMBH growth at high- z than the CDM model, but that the predictions for low- z are very similar. The light-seed case is more sensitive to the DM model since it relies more on the merging of light halos for the build-up of the seeds. If lighter FDM masses are considered, the same problem affects the heavy-seed case, as shown by the dotted curve.

Results – We perform a Markov-chain Monte Carlo (MCMC) analysis over the model parameters $\theta = (m_{\text{seed}}, M_{\text{seed}}, f_{\text{SN}}, f_1^{\text{acc}}, f_2^{\text{acc}}, f_{\text{Edd}}, p_{\text{BH}}, m_{\text{FDM/WDM}})$ defined in Table I, comparing the predictions in the m_{BH}, M_* plane at each redshift to the observations [12–20, 54, 55]. In each case, we generate four MCMC chains of 2×10^4 steps with 5×10^3 steps burn-in, and check the convergence of the chains using the Gelman-Rubin statistic [56]. The likelihood is given by

$$\mathcal{L}(\theta) \propto \prod_j \int d \log_{10} m_{\text{BH}} d \log_{10} M_* \frac{dP(m_{\text{BH}}|M_*, z_j, \theta)}{d \log_{10} m_{\text{BH}}} \times \mathcal{N}(\log_{10} m_{\text{BH}} | \log_{10} m_{\text{BH},j}, \sigma_{\text{BH},j}) \times \mathcal{N}(\log_{10} M_* | \log_{10} M_{*,j}, \sigma_{*,j}), \quad (11)$$

where j labels the data points, and the Gaussian probability densities $\mathcal{N}(x|\bar{x}, \sigma)$ account for the uncertainties in the measurements of the BH masses and the galaxy stellar masses. For each parameter, we consider log-uniform priors.

We display in Fig. 4 the 68.5% and 95.4% contours of the posteriors in a CDM universe. We see a strong cor-

relation between m_{seed} and M_{seed} , which is qualitatively compatible with the findings of [28]. Both the light- and heavy-seed scenarios can provide good fits, but for light seeds of $m_{\text{seed}} < 10^4 M_\odot$ they need to be planted in very light halos, $M_{\text{seed}} \lesssim 10^6 M_\odot$. Whether such initial conditions are physical is up for debate. Some studies have found such light halos to be able to host Pop-III stars [57], although the majority of studies find higher halo mass thresholds [58, 59]. The grey band in the marginalised posterior for M_{seed} indicates the range of predictions from these studies, we can see that it falls within the 68.5 % confidence level (CL) region.

We see that light seeds require a high efficiency of mergers, $p_{\text{BH}} \simeq 1$ while for heavy seeds the preference is for $p_{\text{BH}} \simeq 0.1$. Low values of $p_{\text{BH}} \lesssim 0.1$ are excluded at the 68.5 % CL. The grey band in the marginalised posterior for p_{BH} indicates the range that reproduces the observed PTA GW background when environmental effects on the SMBH binary evolution are taken into account [61]. Considering SMBH binaries driven solely by GW emission prefers $p_{\text{BH}} \sim 0.17$ [61], which, as mentioned above, would indicate a preference for heavy seeds.

We find an upper bound of $f_{\text{SN}} < 10^{-2.21}$ at the 68.5 % CL on the efficiency of the SN feedback. If f_{SN} is too large, the SMBHs can accrete efficiently at all masses. This results in a power-law stellar mass-SMBH mass relation that does not give a good fit for the local AGNs, as has been seen in simulations that suppress the SN feedback [62]. The other accretion parameters $f_1^{\text{acc}}, f_2^{\text{acc}}$ and f_{Edd} are less constrained. We display with red dashed lines the reference value used in [60] to match the AGN luminosity function. We can see that, as expected, there is a preference for either Eddington growth or super-Eddington growth. The correlation with the seed mass is not as strong as with p_{BH} , but we can see that the heavy seed does not have a preference for super-Eddington growth.

We perform similar analyses of the FDM and WDM cases, in which we do not consider changes in the accretion model [65], only in the type of DM, which affects structure evolution. The resulting posteriors are shown in Fig. 5. We find lower bounds on the FDM and WDM masses that depend on the SMBH seed mass: The lighter the seeds are, the higher the FDM or WDM mass has to be. The same correlation between m_{seed} and p_{BH} that we found in the CDM case holds here, and the smaller the merging efficiency, the less stringent the DM mass bounds are. Marginalising over all the parameters, we find that $m_{\text{FDM}} < 2.0 \times 10^{-20}$ eV and $m_{\text{WDM}} < 7.2$ keV are excluded at the 95% CL. If the correct scenario for seeding is light seeds, something that could be tested with future GW detectors [50], then the bounds would become much more stringent.

In the case of FDM, the bound is as stringent as the bound coming from Lyman- α , which implies $m_{\text{FDM}} > 2 \times 10^{-20}$ eV [66]. Other cosmological and astrophysical bounds include $m_{\text{FDM}} > 0.6 \times 10^{-19}$ eV from Eridanus II [67], $m_{\text{FDM}} \gtrsim 3 \times 10^{-19}$ eV from Segue 1 and

² Since we treat the mergers as instantaneous, all the seeds in the small halos are combined in a bigger galaxy and SMBH. In a more realistic model, this process will take time, and not all the SMBHs in the proto-galaxies may combine into a big central SMBH. We plan to explore this further in future work.

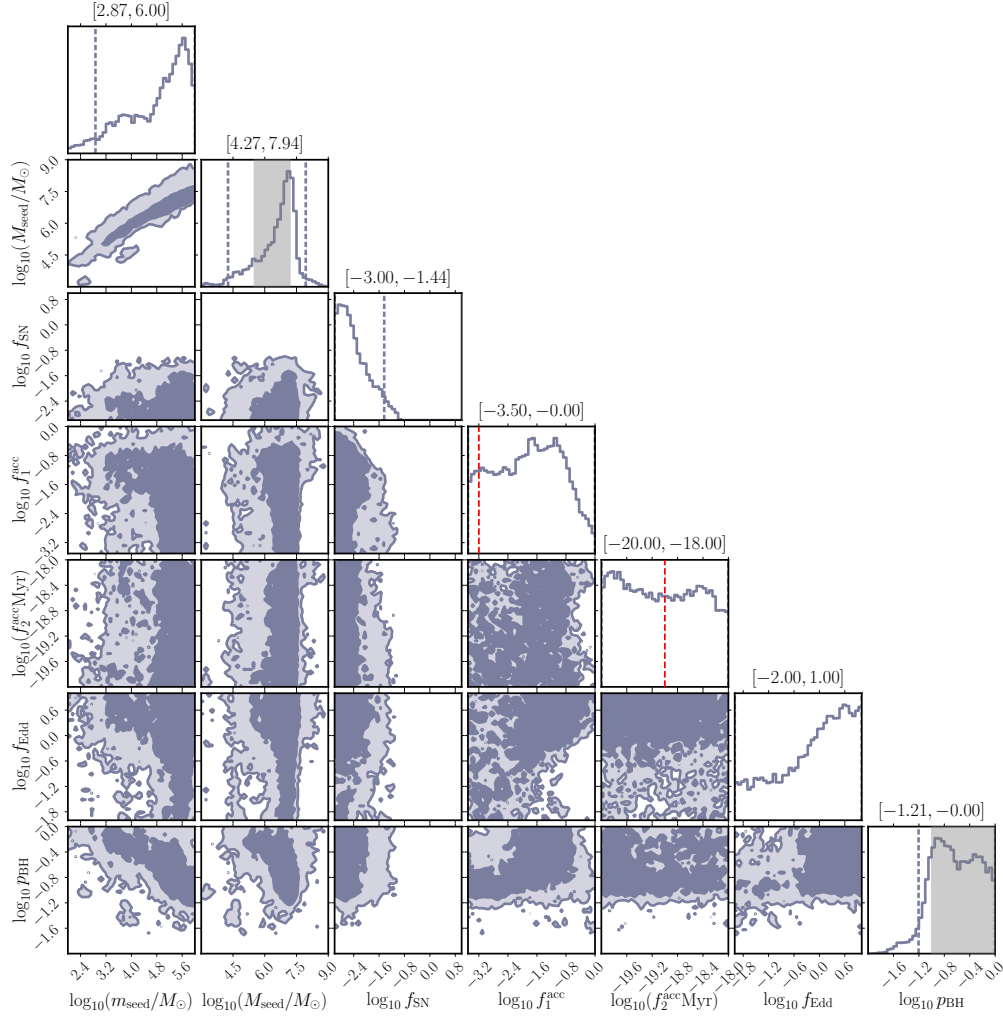


FIG. 4. Posteriors of the stellar mass-BH mass relation fit in a CDM universe. The contours indicate the 68% and 95% credible regions. The grey dashed region in the $\log_{10}(M_{\text{seed}}/M_{\odot})$ posterior represents the range of values given in the literature for this parameter [57–59], the two red dashed lines correspond to the values given in [60] to match the AGN luminosity function and finally the grey range on p_{BH} is the range that gives the correct PTA strength according to [61].

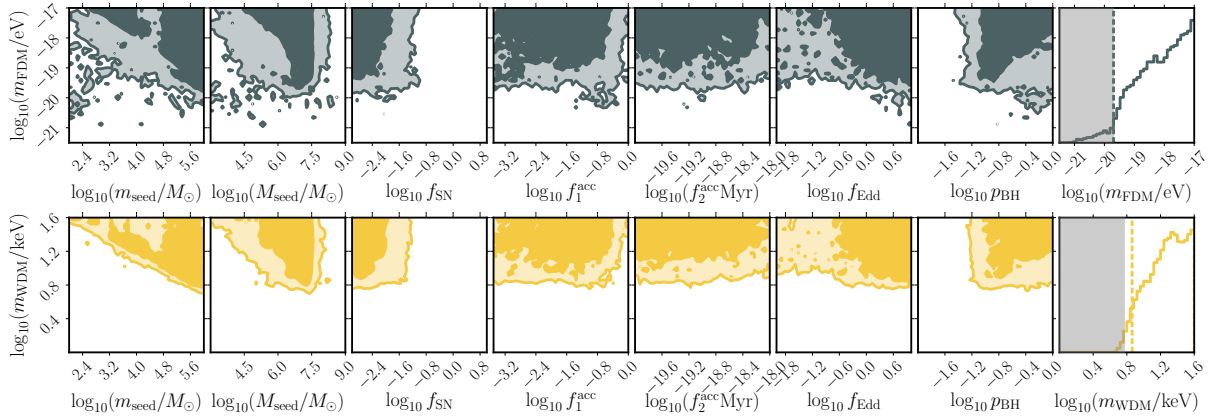


FIG. 5. Posteriors of the stellar mass/BH mass fit parameters as functions of the FDM (upper panels) and WDM (lower panels) masses. The vertical dashed lines are our 95% CL lower bounds on these masses. The grey band in the $\log_{10}(m_{\text{FDM}}/\text{eV})$ posterior shows the most stringent 95% CL exclusion of m_{FDM} from a Lyman- α analysis [63], namely $< 2 \times 10^{-20}$ eV, and the grey band in the $\log_{10}(m_{\text{WDM}}/\text{keV})$ posterior shows the most stringent 95% CL exclusion of m_{WDM} from a joint analysis of strong gravitational lensing, the Lyman- α forest and Milky Way satellites [64], namely < 6.0 keV.

2 [68], $m_{\text{FDM}} \gtrsim 2.2 \times 10^{21}$ eV from Cetus-II [69], and $m_{\text{FDM}} > 4.4 \times 10^{-21}$ eV from gravitational lensing [70]. Some works suggest evidence for FDM with $m_{\text{FDM}} \lesssim 10^{-22}$ eV [71, 72], which conflicts with these limits. As a function of the SMBH seed mass, the lower bounds are approximately $m_{\text{FDM}} \gtrsim 10^{-20}$ eV $(m_{\text{seed}}/10^6 M_{\odot})^{-3/4}$.

For the WDM case we find a very similar behaviour, and the current SMBH population implies $m_{\text{WDM}} > 7.2$ keV, which is slightly more stringent than the bound coming from a combined analysis of strong gravitational lensing, Lyman- α and Milky Way satellites [64] of $m_{\text{WDM}} > 6.0$ keV. Again we see a correlation with the seeding mass of the form $m_{\text{WDM}} \gtrsim 10^{0.7} \text{ keV } (m_{\text{seed}}/10^6 M_{\odot})^{-0.225}$. Other constraints include: $m_{\text{WDM}} > 5.3$ keV from Ly α data [73], $m_{\text{WDM}} > 0.8$ keV from lensing at $z \sim 0.2$ [74], $m_{\text{WDM}} > 5.6$ keV from quasar lensing [75], $m_{\text{WDM}} > 3.0$ keV from quadruple-image lenses [76], $m_{\text{WDM}} > 3.6$ keV from Milky Way satellites [77], and $m_{\text{WDM}} > 3.2$ keV from JWST UV luminosity data [78].

Conclusions – We have found that SMBHs could be better discriminators of DM scenarios than stars [48]. The reason is that, while stars are short-lived, SMBHs live practically forever. Consequently, the SMBH population retains imprints of their seeding scenario. Since seeding occurred at very high redshifts in low-mass halos, these imprints are ideal for testing deviations from CDM.

Leveraging this insight, we have used the latest data from the JWST on both the stellar population, which informs the internal galactic processes, and the masses of the galaxies that host the SMBH, in conjunction with

previous data, to put new bounds on DM. We have found that FDM masses of $m_{\text{FDM}} < 2.0 \times 10^{-20}$ eV and WDM masses of $m_{\text{WDM}} < 7.2$ keV are excluded at the 95% CL.

We have also studied the plausibility of the SMBH growth model against the observed SMBH population. We have found that the JWST population can be accommodated and that the best-fit parameters fall within the range of expected values from simulations, physical arguments, as well as the PTA GW background strength. We also find that the feasibility of light seeds does not depend only on their ability to grow at super-Eddington rates (which is favoured but not required), but on whether they are planted in sufficiently light halos. These protogalaxies will eventually be trapped in an overdensity, which will cause the small galaxies to merge into a bigger one. If the SMBHs that take part can merge efficiently enough, they can become viable seeding candidates. This makes the bounds on DM dependent on the seeding scenario, and light seeds provide more stringent bounds on deviations from CDM. This is an interesting phenomenon that could be explored with future gravitational wave detectors such as LISA [49] and AION [50].

Acknowledgments – This work was supported by the Estonian Research Council grants PRG803, PSG869, RVTT3 and RVTT7 and the Center of Excellence program TK202. The work of J.E. and M.F. was supported by the United Kingdom STFC Grants ST/T000759/1 and ST/T00679X/1. The work of V.V. was partially supported by the European Union’s Horizon Europe research and innovation program under the Marie Skłodowska-Curie grant agreement No. 101065736.

-
- [1] S.L. Finkelstein, M.B. Bagley, P. Arrabal Haro, M. Dickinson, H.C. Ferguson, J.S. Kartaltepe et al., *The Cosmic Evolution Early Release Science Survey (CEERS)*, *ApJ* **983** (2025) L4 [2501.04085].
 - [2] C.T. Donnan, R.J. McLure, J.S. Dunlop, D.J. McLeod, D. Magee, K.Z. Arellano-Córdova et al., *JWST PRIMER: a new multifield determination of the evolving galaxy UV luminosity function at redshifts $z = 9 - 15$* , *MNRAS* **533** (2024) 3222 [2403.03171].
 - [3] M.B. Bagley, N. Pirzkal, S.L. Finkelstein, C. Papovich, D.A. Berg, J.M. Lotz et al., *The Next Generation Deep Extragalactic Exploratory Public (NGDEEP) Survey*, *ApJ* **965** (2024) L6 [2302.05466].
 - [4] C.M. Casey, J.S. Kartaltepe, N.E. Drakos, M. Franco, S. Harish, L. Paquereau et al., *COSMOS-Web: An Overview of the JWST Cosmic Origins Survey*, *ApJ* **954** (2023) 31 [2211.07865].
 - [5] D.J. Eisenstein, C. Willott, S. Alberts, S. Arribas, N. Bonaventura, A.J. Bunker et al., *Overview of the JWST Advanced Deep Extragalactic Survey (JADES)*, *arXiv e-prints* (2023) arXiv:2306.02465 [2306.02465].
 - [6] M.J. Rieke, B. Robertson, S. Tacchella, K. Hainline, B.D. Johnson, R. Hausen et al., *JADES Initial Data Release for the Hubble Ultra Deep Field: Revealing the Faint Infrared Sky with Deep JWST NIRCам Imaging*, *ApJS* **269** (2023) 16 [2306.02466].
 - [7] G. Östlin et al., *MIRI Deep Imaging Survey (MIDIS) of the Hubble Ultra Deep Field - Survey description and early results for the galaxy population detected at 5.6 μm* , *Astron. Astrophys.* **696** (2025) A57 [2411.19686].
 - [8] R. Bezanson, I. Labbe, K.E. Whitaker, J. Leja, S.H. Price, M. Franx et al., *The JWST UNCOVER Treasury Survey: Ultradeep NIRSpect and NIRCам Observations before the Epoch of Reionization*, *ApJ* **974** (2024) 92 [2212.04026].
 - [9] A. Adamo, H. Atek, M.B. Bagley, E. Bañados, K.S.S. Barrow, D.A. Berg et al., *The first billion years according to JWST*, *Nature Astronomy* (2025) [2405.21054].
 - [10] M. Volonteri, M. Habouzit and M. Colpi, *The origins of massive black holes*, *Nature Rev. Phys.* **3** (2021) 732 [2110.10175].
 - [11] V. Cammelli, P. Monaco, J.C. Tan, J. Singh, F. Fontanot, G. De Lucia et al., *The formation of supermassive black holes from Population III.1 seeds. III. Galaxy evolution and black hole growth from semi-analytic modelling*, *MNRAS* **536** (2025) 851 [2407.09949].

- [12] X. Ding, M. Onoue, J.D. Silverman, Y. Matsuoka, T. Izumi, M.A. Strauss et al., *Detection of stellar light from quasar host galaxies at redshifts above 6*, *Nature* **621** (2023) 51 [2211.14329].
- [13] H. Übler, R. Maiolino, E. Curtis-Lake, P.G. Pérez-González, M. Curti, M. Perna et al., *GA-NIFS: A massive black hole in a low-metallicity AGN at $z \sim 5.55$ revealed by JWST/NIRSpec IFS*, *A&A* **677** (2023) A145 [2302.06647].
- [14] R.L. Larson, S.L. Finkelstein, D.D. Kocevski, T.A. Hutchison, J.R. Trump, P. Arrabal Haro et al., *A CEERS Discovery of an Accreting Supermassive Black Hole 570 Myr after the Big Bang: Identifying a Progenitor of Massive $z \gtrsim 6$ Quasars*, *ApJ* **953** (2023) L29 [2303.08918].
- [15] Y. Harikane, Y. Zhang, K. Nakajima, M. Ouchi, Y. Isobe, Y. Ono et al., *A JWST/NIRSpec First Census of Broad-line AGNs at $z = 4\text{--}7$: Detection of 10 Faint AGNs with $M_{\text{BH}} 10^6\text{--}10^8 M_{\odot}$ and Their Host Galaxy Properties*, *ApJ* **959** (2023) 39 [2303.11946].
- [16] A. Bogdan et al., *Evidence for heavy-seed origin of early supermassive black holes from a $z \approx 10$ X-ray quasar*, *Nature Astron.* **8** (2024) 126 [2305.15458].
- [17] R. Maiolino et al., *JADES - The diverse population of infant black holes at $4 < z < 11$: Merging, tiny, poor, but mighty*, *Astron. Astrophys.* **691** (2024) A145 [2308.01230].
- [18] M. Yue, A.-C. Eilers, R.A. Simcoe, R. Mackenzie, J. Matthee, D. Kashino et al., *EIGER. V. Characterizing the Host Galaxies of Luminous Quasars at $z \gtrsim 6$* , *ApJ* **966** (2024) 176 [2309.04614].
- [19] D.D. Kocevski, M. Onoue, K. Inayoshi, J.R. Trump, P. Arrabal Haro, A. Grazian et al., *Hidden Little Monsters: Spectroscopic Identification of Low-mass, Broad-line AGNs at $z \gtrsim 5$ with CEERS*, *ApJ* **954** (2023) L4 [2302.00012].
- [20] M.A. Stone, J. Lyu, G.H. Rieke, S. Alberts and K.N. Hainline, *Undermassive Host Galaxies of Five $z \sim 6$ Luminous Quasars Detected with JWST*, *ApJ* **964** (2024) 90 [2310.18395].
- [21] F. Pacucci, B. Nguyen, S. Carniani, R. Maiolino and X. Fan, *JWST CEERS and JADES Active Galaxies at $z = 4\text{--}7$ Violate the Local $M - M_{\star}$ Relation at $\gtrsim 3\sigma$: Implications for Low-mass Black Holes and Seeding Models*, *ApJ* **957** (2023) L3 [2308.12331].
- [22] J. Ellis, M. Fairbairn, G. Hütsi, J. Urrutia, V. Vaskonen and H. Veermäe, *Consistency of JWST black hole observations with NANOGrav gravitational wave measurements*, *Astron. Astrophys.* **691** (2024) A270 [2403.19650].
- [23] J. Li, J.D. Silverman, Y. Shen, M. Volonteri, K. Jahnke, M.-Y. Zhuang et al., *Tip of the Iceberg: Overmassive Black Holes at $4 \leq z \leq 7$ Found by JWST Are Not Inconsistent with the Local Relation*, *ApJ* **981** (2025) 19 [2403.00074].
- [24] P. Dayal and R. Maiolino, *The properties of primordially-seeded black holes and their hosts in the first billion years: implications for JWST*, *arXiv e-prints* (2025) arXiv:2506.08116 [2506.08116].
- [25] P. Natarajan, F. Pacucci, A. Ricarte, A. Bogdan, A.D. Goulding and N. Cappelluti, *First Detection of an Overmassive Black Hole Galaxy UHZ1: Evidence for Heavy Black Hole Seed Formation from Direct Collapse*, *ApJ* **960** (2024) L1 [2308.02654].
- [26] A. Toubiana, L. Sberna, M. Volonteri, E. Barausse, S. Babak, R. Enficiaud et al., *Reconciling PTA and JWST and preparing for LISA with POMPOCO: a Parametrisation Of the Massive black hole POpulation for Comparison to Observations*, *Astron. Astrophys.* **700** (2025) A135 [2410.17916].
- [27] D.D. Kocevski, S.L. Finkelstein, G. Barro, A.J. Taylor, A. Calabrò, B. Laloux et al., *The Rise of Faint, Red Active Galactic Nuclei at $z \gtrsim 4$: A Sample of Little Red Dots in the JWST Extragalactic Legacy Fields*, *ApJ* **986** (2025) 126 [2404.03576].
- [28] J. Ellis, M. Fairbairn, J. Urrutia and V. Vaskonen, *What is the origin of the JWST SMBHs?*, **2410.24224**.
- [29] A.K. Bhowmick, L. Blecha, P. Torrey, L.Z. Kelley, R. Weinberger, M. Vogelsberger et al., *Introducing the BRAHMA simulation suite: signatures of low-mass black hole seeding models in cosmological simulations*, *MNRAS* **531** (2024) 4311 [2402.03626].
- [30] K. Kritos, R.S. Beckmann, J. Silk, E. Berti, S. Yi, M. Volonteri et al., *Supermassive black hole growth in hierarchically merging nuclear star clusters*, **2412.15334**.
- [31] O. Pian, H.-Y. Pu and K. Wu, *Super-Eddington accretion in high-redshift black holes and the emergence of jetted AGN*, *MNRAS* **530** (2024) 1732 [2403.15106].
- [32] A. Lupi, A. Trinca, M. Volonteri, M. Dotti and C. Mazzucchelli, *Size matters: are we witnessing super-Eddington accretion in high-redshift black holes from JWST?*, *Astron. Astrophys.* **689** (2024) A128 [2406.17847].
- [33] E. Lambrides et al., *The Case for Super-Eddington Accretion: Connecting Weak X-ray and UV Line Emission in JWST Broad-Line AGN During the First Gyr of Cosmic Time*, **2409.13047**.
- [34] P. Madau, *Chasing the Light: Shadowing, Collimation, and the Super-Eddington Growth of Infant Black Holes in JWST-Discovered AGNs*, **2501.09854**.
- [35] T. Zana, P.R. Capelo, M. Boresta, R. Schneider, A. Lupi, A. Trinca et al., *Super-Eddington accretion in protogalactic cores*, **2508.21114**.
- [36] J. Yang, F. Wang, X. Fan, J.F. Hennawi, A.J. Barth, E. Bañados et al., *A Spectroscopic Survey of Biased Halos in the Reionization Era (ASPIRE): A First Look at the Rest-frame Optical Spectra of $z \gtrsim 6.5$ Quasars Using JWST*, *ApJ* **951** (2023) L5 [2304.09888].
- [37] A.J. Taylor, S.L. Finkelstein, D.D. Kocevski, J. Jeon, V. Bromm, R.O. Amorín et al., *Broad-line AGNs at $3.5 \leq z \leq 6$: The Black Hole Mass Function and a Connection with Little Red Dots*, *ApJ* **986** (2025) 165 [2409.06772].
- [38] J.E. Greene, I. Labbé, A.D. Goulding, L.J. Furtak, I. Chemerynska, V. Kokorev et al., *UNCOVER Spectroscopy Confirms the Surprising Ubiquity of Active Galactic Nuclei in Red Sources at $z \gtrsim 5$* , *ApJ* **964** (2024) 39 [2309.05714].
- [39] J. Matthee et al., *Little Red Dots: An Abundant Population of Faint Active Galactic Nuclei at $z \sim 5$ Revealed by the EIGER and FRESCO JWST Surveys*, *ApJ* **963** (2024) 129 [2306.05448].
- [40] X. Shen, M. Vogelsberger, M. Boylan-Kolchin, S. Tacchella and R.P. Naidu, *Early galaxies and early dark energy: a unified solution to the hubble tension and puzzles of massive bright galaxies revealed by JWST*, *MNRAS* **533** (2024) 3923 [2406.15548].

- [41] F. Gentile et al., *Not-so-little Red Dots: Two Massive and Dusty Starbursts at $z \sim 5-7$ Pushing the Limits of Star Formation Discovered by JWST in the COSMOS-Web Survey*, *ApJ* **973** (2024) L2 [2408.10305].
- [42] M. Kokubo and Y. Harikane, *Challenging the AGN scenario for JWST/NIRSpec broad H α emitters/Little Red Dots in light of non-detection of NIRCам photometric variability and X-ray*, *2407.04777*.
- [43] T.T. Ananna, Á. Bogdán, O.E. Kovács, P. Natarajan and R.C. Hickox, *X-Ray View of Little Red Dots: Do They Host Supermassive Black Holes?*, *ApJ* **969** (2024) L18 [2404.19010].
- [44] P. Madau and F. Haardt, *X-Ray Weak Active Galactic Nuclei from Super-Eddington Accretion onto Infant Black Holes*, *ApJ* **976** (2024) L24 [2410.00417].
- [45] F. Pacucci and R. Narayan, *Mildly Super-Eddington Accretion onto Slowly Spinning Black Holes Explains the X-Ray Weakness of the Little Red Dots*, *ApJ* **976** (2024) 96 [2407.15915].
- [46] R.P. Naidu et al., *A "Black Hole Star" Reveals the Remarkable Gas-Enshrouded Hearts of the Little Red Dots*, *2503.16596*.
- [47] I. Juodžbalis, C. Marconcini, F. D'Eugenio, R. Maiolino, A. Marconi, H. Übler et al., *A direct black hole mass measurement in a little red dot at the epoch of reionization*, *arXiv:2508.21748*, 2025.
- [48] J. Ellis, M. Fairbairn, J. Urrutia and V. Vaskonen, *Starlight from JWST: Implications for star formation and dark matter models*, *2504.20043*.
- [49] LISA collaboration, *LISA Definition Study Report*, *2402.07571*.
- [50] AION collaboration, *A Prototype Atom Interferometer to Detect Dark Matter and Gravitational Waves*, *2504.09158*.
- [51] D. Mukherjee, Y. Zhou, N. Chen, U.N. Di Carlo and T. Di Matteo, *MAGICs. III. Seeds Sink Swiftly: Nuclear Star Clusters Dramatically Accelerate Seed Black Hole Mergers*, *ApJ* **981** (2025) 203 [2409.19095].
- [52] P. Dayal, E.M. Rossi, B. Shiralilou, O. Piana, T.R. Choudhury and M. Volonteri, *The hierarchical assembly of galaxies and black holes in the first billion years: predictions for the era of gravitational wave astronomy*, *MNRAS* **486** (2019) 2336 [1810.11033].
- [53] A.K. Bhowmick, L. Blecha, L.Z. Kelley, A. Sivasankaran, P. Torrey, R. Weinberger et al., *Dynamics of low-mass black hole seeds in the BRAHMA simulations using subgrid-dynamical friction: Impact on merger-driven black hole growth in the high redshift Universe*, *arXiv e-prints* (2025) arXiv:2506.09184 [2506.09184].
- [54] A.E. Reines and M. Volonteri, *Relations between Central Black Hole Mass and Total Galaxy Stellar Mass in the Local Universe*, *ApJ* **813** (2015) 82 [1508.06274].
- [55] T. Izumi, Y. Matsuoka, S. Fujimoto, M. Onoue, M.A. Strauss, H. Umehata et al., *Subaru High- z Exploration of Low-luminosity Quasars (SHELLQs). XIII. Large-scale Feedback and Star Formation in a Low-luminosity Quasar at $z = 7.07$ on the Local Black Hole to Host Mass Relation*, *ApJ* **914** (2021) 36 [2104.05738].
- [56] A. Gelman and D.B. Rubin, *Inference from Iterative Simulation Using Multiple Sequences*, *Statist. Sci.* **7** (1992) 457.
- [57] S. Naoz and R. Barkana, *The formation and gas content of high-redshift galaxies and minihaloes*, *MNRAS* **377** (2007) 667 [astro-ph/0612004].
- [58] A.T.P. Schauer, S.C.O. Glover, R.S. Klessen and P. Clark, *The influence of streaming velocities and Lyman-Werner radiation on the formation of the first stars*, *MNRAS* **507** (2021) 1775 [2008.05663].
- [59] M. Kulkarni, E. Visbal and G.L. Bryan, *The Critical Dark Matter Halo Mass for Population III Star Formation: Dependence on Lyman-Werner Radiation, Baryon-dark Matter Streaming Velocity, and Redshift*, *ApJ* **917** (2021) 40 [2010.04169].
- [60] P. Dayal, E.M. Rossi, B. Shiralilou, O. Piana, T.R. Choudhury and M. Volonteri, *The hierarchical assembly of galaxies and black holes in the first billion years: predictions for the era of gravitational wave astronomy*, *MNRAS* **486** (2019) 2336 [1810.11033].
- [61] J. Ellis, M. Fairbairn, G. Hütsi, J. Raidal, J. Urrutia, V. Vaskonen et al., *Gravitational waves from supermassive black hole binaries in light of the NANOGrav 15-year data*, *Phys. Rev. D* **109** (2024) L021302 [2306.17021].
- [62] R.G. Bower, J. Schaye, C.S. Frenk, T. Theuns, M. Schaller, R.A. Crain et al., *The dark nemesis of galaxy formation: why hot haloes trigger black hole growth and bring star formation to an end*, *MNRAS* **465** (2017) 32 [1607.07445].
- [63] V. Iršič, M. Viel, M.G. Haehnelt, J.S. Bolton and G.D. Becker, *First constraints on fuzzy dark matter from Lyman- α forest data and hydrodynamical simulations*, *Phys. Rev. Lett.* **119** (2017) 031302 [1703.04683].
- [64] W. Enzi et al., *Joint constraints on thermal relic dark matter from strong gravitational lensing, the Ly α forest, and Milky Way satellites*, *MNRAS* **506** (2021) 5848 [2010.13802].
- [65] H.H.S. Chiu, H.-Y. Schive, H.-Y.K. Yang, H. Huang and M. Gaspari, *Boosting Supermassive Black Hole Growth in the Early Universe by Fuzzy Dark Matter Solitons*, *Phys. Rev. Lett.* **134** (2025) 051402 [2501.09098].
- [66] K.K. Rogers and H.V. Peiris, *Strong Bound on Canonical Ultralight Axion Dark Matter from the Lyman-Alpha Forest*, *Phys. Rev. Lett.* **126** (2021) 071302 [2007.12705].
- [67] D.J.E. Marsh and J.C. Niemeyer, *Strong Constraints on Fuzzy Dark Matter from Ultrafaint Dwarf Galaxy Eridanus II*, *Phys. Rev. Lett.* **123** (2019) 051103 [1810.08543].
- [68] N. Dalal and A. Kravtsov, *Excluding fuzzy dark matter with sizes and stellar kinematics of ultrafaint dwarf galaxies*, *Phys. Rev. D* **106** (2022) 063517 [2203.05750].
- [69] M. Benito, G. Hütsi, K. Müirsepp, J.S. Almeida, J. Urrutia, V. Vaskonen et al., *Fuzzy dark matter fails to explain dark matter cores*, *Phys. Dark Univ.* **49** (2025) 102010 [2502.12030].
- [70] D.M. Powell, S. Vegetti, J.P. McKean, S.D.M. White, E.G.M. Ferreira, S. May et al., *A lensed radio jet at milli-arcsecond resolution – II. Constraints on fuzzy dark matter from an extended gravitational arc*, *MNRAS* **524** (2023) L84 [2302.10941].
- [71] A. Amruth et al., *Einstein rings modulated by wavelike dark matter from anomalies in gravitationally lensed images*, *Nature Astron.* **7** (2023) 736 [2304.09895].

- [72] K.K. Rogers and V. Poulin, *5 σ tension between Planck cosmic microwave background and eBOSS Lyman-alpha forest and constraints on physics beyond Λ CDM*, *Phys. Rev. Res.* **7** (2025) L012018 [[2311.16377](#)].
- [73] V. Iršič et al., *New Constraints on the free-streaming of warm dark matter from intermediate and small scale Lyman- α forest data*, *Phys. Rev. D* **96** (2017) 023522 [[1702.01764](#)].
- [74] S. Vegetti, G. Despali, M.R. Lovell and W. Enzi, *Constraining sterile neutrino cosmologies with strong gravitational lensing observations at redshift $z \sim 0.2$* , *MNRAS* **481** (2018) 3661 [[1801.01505](#)].
- [75] J.-W. Hsueh, W. Enzi, S. Vegetti, M. Auger, C.D. Fassnacht, G. Despali et al., *SHARP – VII. New constraints on the dark matter free-streaming properties and substructure abundance from gravitationally lensed quasars*, *MNRAS* **492** (2020) 3047 [[1905.04182](#)].
- [76] D. Gilman, S. Birrer, A. Nierenberg, T. Treu, X. Du and A. Benson, *Warm dark matter chills out: constraints on the halo mass function and the free-streaming length of dark matter with eight quadruple-image strong gravitational lenses*, *MNRAS* **491** (2020) 6077 [[1908.06983](#)].
- [77] A. Dekker, S. Ando, C.A. Correa and K.C.Y. Ng, *Warm dark matter constraints using Milky Way satellite observations and subhalo evolution modeling*, *Phys. Rev. D* **106** (2022) 123026 [[2111.13137](#)].
- [78] B. Liu, H. Shan and J. Zhang, *New Galaxy UV Luminosity Constraints on Warm Dark Matter from JWST*, *ApJ* **968** (2024) 79 [[2404.13596](#)].

Constraints on Dark Matter Models from Supermassive Black Hole Evolution

John Ellis, Malcolm Fairbairn, Juan Urrutia and Ville Vaskonen

SUPPLEMENTAL MATERIAL

We present here corner plots showing the complete posteriors from fits to the stellar mass and BH mass in Fuzzy Dark Matter and Warm Dark Matter cosmologies.

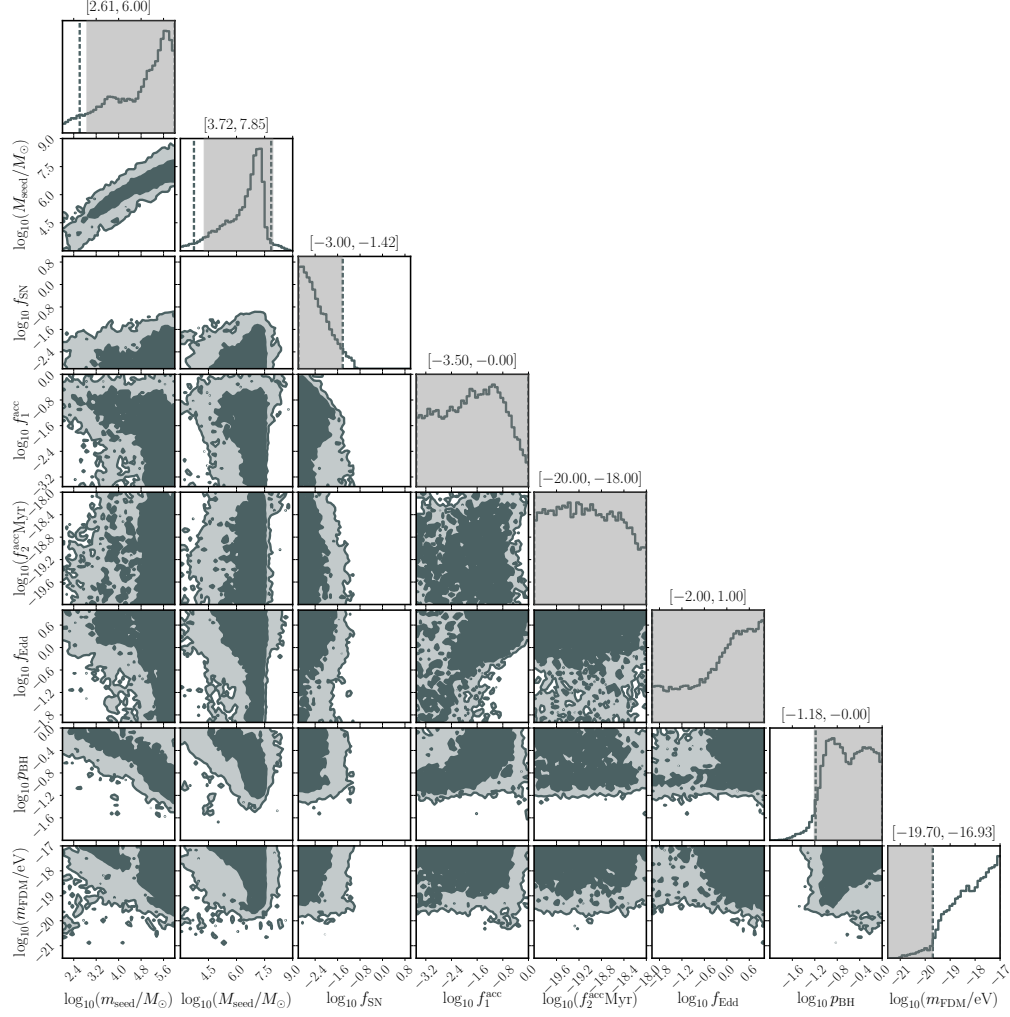


FIG. S1. The posteriors for the stellar mass/BH mass fit parameters are shown as functions of the FDM mass, with the dashed lines represent the 95 % CL of each variable. In the $\log_{10}(m_{\text{FDM}}/\text{eV})$ panel, the grey band marks the 95% CL constraint on m_{FDM} from an analysis of Lyman- α data [63], which excludes masses below 2×10^{-20} eV. The grey bands show the 95% CL ranges the CDM fit.

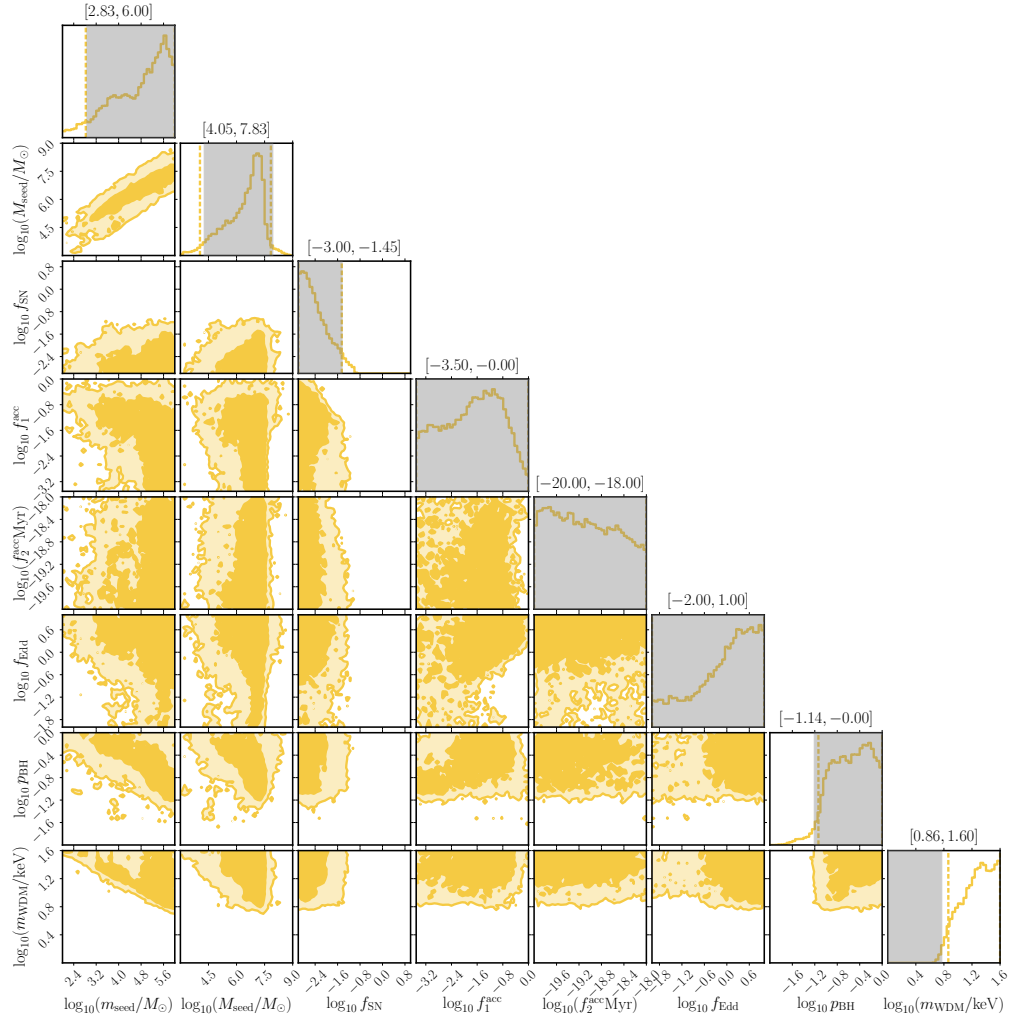


FIG. S2. The posteriors for the stellar mass/BH mass fit parameters are shown as functions of the WDM mass, with the dashed lines representing the 95 % CL of each variable. In the $\log_{10}(m_{\text{WDM}}/\text{keV})$ panel, the grey band marks the 95% CL constraint on m_{WDM} from a joint analysis of strong gravitational lensing, the Lyman- α forest and Milky Way satellites [64], which excludes masses below 6.0 keV. The grey bands show the 95% CL ranges of the CDM fit.